Vertical Structure of P-Band Temporal Decorrelation at the Paracou Forest: Results From TropiScat

Dinh Ho Tong Minh, Stefano Tebaldini, Fabio Rocca, Thuy Le Toan, Pierre Borderies, Thierry Koleck, Clement Albinet, Alia Hamadi, and Ludovic Villard

I. Introduction

THE BIOMASS Monitoring Mission for Carbon Assessment (BIOMASS) has been selected in May 2013 by the European Space Agency to become the seventh Earth Explorer mission, which is scheduled for launch for the 2019–2020 time frame. The satellite will be designed to provide, for the first time from space, P-band radar measurements that are optimized to determine the amount of biomass and carbon stored in the world's forests. This information, which is poorly known in the tropics, is essential to our understanding of the role of forests in Earth's carbon cycle and climate change. During the preparatory phase, the assessment of retrieval methods for measuring above-ground biomass in tropical forests is one of the major research activities [1], [2]. The satellite carries a single sensor, i.e., a P-band (435 MHz, a wavelength of $\sim$69 cm) SAR system. The BIOMASS P-band SAR has full polarimetric and multipass interferometric capabilities. The signal bandwidth is 6 MHz, which is a small value that is constrained by the frequency spectrum allocation.

The BIOMASS mission will last five years and comprise a tomographic phase that is followed by the nominal operational phase. In order to minimize the temporal decorrelation of interferometric acquisitions, an optional observation concept with a repeat cycle as low as three or four days has been studied. The tomographic phase will be performed just after the commissioning phase, which will be carried out with the satellite flying in the nominal orbit or in the tomographic orbit, depending on the final mission design. During this phase, the system will gather multiple acquisitions that are characterized by small baselines and a repeat cycle on the order of a few days, allowing SAR tomography imaging. This phase is expected to directly provide useful inputs for the nominal phase. However, there are three main factors that are expected to have significant impact on the quality of the results. One is the 6-MHz limit that is allowed for the pulse bandwidth, resulting in a severe limit to the vertical resolution if not properly accounted for [3]. Another factor is the interaction with the ionosphere, which affects the data quality, producing disturbances such as Faraday rotation, residual phase screens, image shifts, and even defocusing [4], [5], which need to be corrected with specific algorithms [6]. Finally, a major factor is the one that is related to temporal decorrelation, resulting from short-term and long-term decorrelation mechanisms within the vegetation [7]. The presence of temporal decorrelation has been shown to constitute a crucial issue in multibaseline applications. Temporal decorrelation can make the retrieval of biophysical parameters from interferometric SAR measurements at X-band or C-band almost unfeasible because of the changes in the electromagnetic profiles and/or the positions of the scatterers with time within the resolution cell [8]. However, in urban scenarios, X- and C-bands are useful for the problem of detecting and localizing a collection of a few point targets by exploiting spaceborne tomography [9], [10].

Manuscript received July 17, 2013; revised September 20, 2013; accepted November 3, 2013.

D. Ho Tong Minh, T. Le Toan, C. Albinet, and L. Villard are with the Centre d'Etudes Spatiales de la Biosphere (CESBIO), 31401 Toulouse, France (e-mail: htmdinhrs@gmail.com).

S. Tebaldini and F. Rocca are with the Dipartimento di Elettronica, Informazione e Bioingegneria, Politecnico di Milano, 20133 Milano, Italy (e-mail: tebaldini@elet.polimi.it; rocca@elet.polimi.it).

P. Borderies and A. Hamadi are with the Office National d'Études et de Recherches Aérospatiales (ONERA), 31055 Toulouse, France (e-mail: Pierre.Borderies@onera.fr).

T. Koleck is with Centre d'Etudes Spatiales de la Biosphere (CESBIO), 31401 Toulouse, France and also with Centre National d'Études Spatiales (CNES), 31401 Toulouse, France (e-mail: Thierry.Koleck@cnes.fr).

At L-band, temporal decorrelation is also a critical factor for polarimetric interferometric SAR inversions [11], which needs to be compensated with a specific model [12]. The employment of P-band is expected to yield better measurements because P-band is foreseen to: 1) experience lower temporal decorrelation [13]; 2) penetrate the ground even on very dense forests [14], [15]; and 3) avoid the saturation phenomena of biomass with respect to radar backscatter [16]. However, up to now, no precise information is available concerning the impact of the repeat time on the performance of forest structure retrieval. In other words, there are no measurements available about the vertical distribution of temporal coherence at P-band, specifically in tropical forests.

During the BIOMASS preparation phase, to assess the retrieval algorithms using the P-band SAR measurements over tropical rain forests, the TropiSAR 2009 airborne campaign and the TropiScat 2011 ground-based experiment have been conducted in Paracou, French Guiana [17], [18]. The TropiSAR data set allowed for the investigation of the forest vertical structure and its connection to the forest biomass at a landscape scale [16], [19]. In order to complement the airborne TropiSAR data set, the TropiScat ground-based experiment was implemented to acquire a well-controlled data set in various seasons and weather conditions, delivering intensity and complex coherence in all polarizations [20]. Such an experimental setup provides 2-D vertical imaging (range–height imaging) resolution capabilities through the coherent combination of the signal from different antennas via tomographic techniques. Therefore, again, by coherently comparing the tomographic images that are taken at different times, it is possible to gain access to the variation of temporal coherence with respect to the forest height.

The aim of this letter is to present the results that are obtained from the TropiScat campaign concerning the short-term and long-term temporal decorrelation within the vegetation layer, leading to a discussion on the dependence of temporal decorrelation with respect to the forest vertical structure.

This letter is organized as follows. The TropiScat tomographic mode experiment is briefly introduced in Section II. Coherence patterns are discussed in Section III. Long-term temporal decorrelation behaviors are shown in Section IV. Conclusions are drawn in Section V.

II. TropiScat Tomographic Mode

The major objective of the TropiScat campaign is the temporal survey of the variation of the radar measurements in time scales ranging from diurnal, weekly, monthly, and up to one year of observation and, possibly, beyond. The measurements include the intensity, coherence, and vertical imaging at all linear polarizations. Concerning the TropiScat tomographic mode, the main goal is the assessment of the vertical distribution of temporal coherence, covering time scales of hours, days, and months.

The Paracou field station is located in a lowland moist tropical forest with high above-ground biomass (up to 450 t/ha) near Sinnamary, French Guiana. In 2003, the Guyaflux metallic tower was built in an existing natural 100-m^2 gap [21]. The 55-m-high Guyaflux tower is about 20 m higher than the overall canopy. The experiment has been successfully set up and operated since October 2011 at this field station, where the equipment was installed on top of the Guyaflux tower to illuminate the forest below [18], [20].

Fig. 1. Antenna positions for the TropiScat tomographic system in the Guyaflux tower. The design encompasses one vertical array of five antennas for each polarization (i.e., horizontal or vertical) and each operating mode (i.e., transmit or receive).

The TropiScat tomographic array has been designed and implemented, as shown in Fig. 1. The system consists of a vector network analyzer that is connected to 20 antennas through a switch box. The transmitted signal occupies the frequency spectrum between 400 and 600 MHz (corresponding to the upper P-band), resulting in a range resolution of 0.75 m.

Fig. 1 shows that the real array antennas are irregularly positioned along the vertical direction. However, by employing multiple transmitting–receiving pairs, a uniform equivalent monostatic array is formed along that direction for each polarimetric channel, resulting in the same tomographic imaging properties in all polarizations. The resulting virtual array aperture and spacing are $A_z = 2.8$ and $dz = 0.2$ m, respectively. At this vertical spacing, the height of ambiguity turns out to be higher than 50 m for a range distance that is > 60 m even at 900 MHz, which is well distinguished from the forest. Furthermore, the virtual array aperture results in the vertical resolution in the far range (70 m), being about 7.5 m in the P-band, and is proportionally finer at higher frequencies. The TropiScat system has no azimuth resolution. As a consequence, the tomographic imaging is relative to an average over an azimuth angular sector. The equipment allows us to gather the signals at the tomographic array within a few minutes, resulting in the possibility of producing a tomographic image of the forest with a temporal sampling of 15 min. For a comprehensive description of the TropiScat campaign and related performance, see [20].

The focus of this letter is on the (P-band) data at 500 MHz, although the data at 700 and 900 MHz are available as well. We have chosen to work on the P-band data because it was decided to be a top priority for the TropiScat campaign, providing input for the BIOMASS mission study. Furthermore, we focus on the near range area (i.e., from 60 to 120 m away from the array) because the vertical resolution is on the order of 6–12 m, which allows us to separately study different vertical layers within the forest volume.

Tomographic processing is carried out to focus all available acquisitions in the range–height plane to form a vertical section of the illuminated forest. All results have been flattened to bring the terrain level at 0 m, in order to help the visualization and interpretation of the results [20].

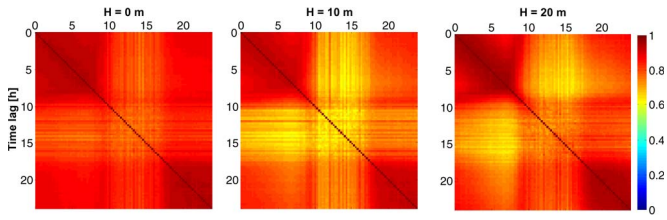

Fig. 2. HV coherency matrix over the average of one day from ten dry days in December 2011.

III. Coherence Matrix Analysis

As aforementioned, the TropiScat experiment makes it possible to produce a vertical section of the illuminated forest every 15 min. This means that it is possible to analyze the temporal behavior of the forest at different heights by evaluating the interferometric coherence between the tomograms that are gathered at different times.

The instrument that is used in this section to perform this analysis is the so-called *coherence matrix*. For a set of N acquisitions, the coherence matrix is defined as the $N \times N$ matrix that is obtained by taking the N^2 interferometric coherence of all available interferometric pairs. Each entry in the coherence matrix has been obtained by taking the interferometric coherence between two different acquisition times at one particular location within the forest.

In the remainder of this letter, we will discuss the temporal behavior at different height locations within the vegetation by considering the coherence matrix that corresponds to each layer.

A. Coherence Over 24 h

Here, we examine the temporal coherence over a time span of 24 h. Fig. 2 shows the HV coherence matrices over one day at the ground layer (0 m) and at 10 and 20 m above the ground. At each layer, for the coherence evaluation, we exploit the samples in the range direction rather than in the height direction. Due to the range resolution of 0.75 m, the coherence evaluation has been carried out by employing an averaging window of 5 $\times$ 40 m (height–range), corresponding to about 50 looks. All the examined coherence matrices were extracted by considering a near range location (about 85 m away from the array), where the vertical resolution is finer. Furthermore, we employ ten dry days in December 2011 to improve the robustness of the coherence estimates.

In Fig. 2, it is observed that the lowest coherence values are associated with the daytime acquisitions. This result is consistent with the defocusing phenomena that are discussed in [20], where it was shown that the daytime acquisitions are perturbed by the action of the wind. It is worth noting that this phenomenon is partly observed at the ground level as a result of defocused contributions from the rest of the vegetation layer. Nighttime acquisitions are instead observed to produce the highest coherence values. However, the most relevant phenomenon is that the nighttime acquisitions yield high coherence values.

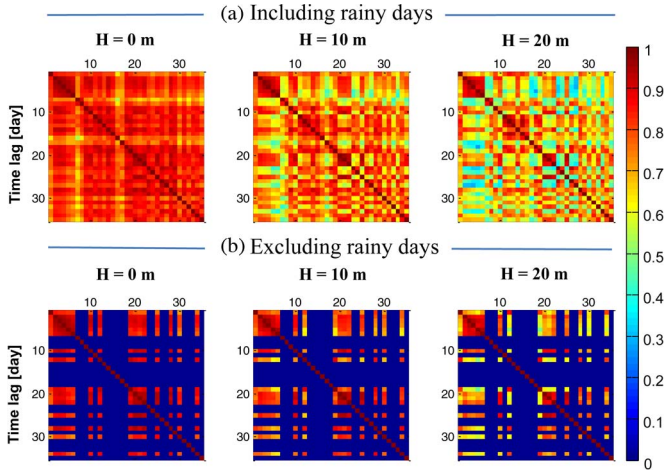

Fig. 3. (a) HV coherency matrices for 35 days at dawn–dawn as a function of the height, including rainy days. (b) HV coherency matrices for 35 days at dawn–dawn as a function of the height, excluding rainy days. The rainy days were flagged by setting their coherence to 0. The data cover the time span starting from December 15, 2011.

This result suggests that the performance over tropical areas can be optimized by gathering the data within a temporal window ranging from approximately 7 P.M. to 7 A.M. However, at P-band, ionospheric disturbances are much stronger at dusk [5]. We decide to focus on the dawn–dawn acquisitions rather than the dusk–dusk acquisitions. The following sections will be focused on the evaluation of the long-term temporal coherence by considering the dawn (6 A.M.) acquisitions.

B. Dawn–Dawn Long-Term Coherence

This section is dedicated to providing a quantitative assessment of the temporal decorrelation at a time scale of days. To this aim, here, we show the complete coherence matrix for 35 days (dawn–dawn).

Fig. 3 shows the coherence matrix at an HV channel as a function of the forest height (0, 10, and 20 m). All acquisitions are gathered at 6 A.M. The considered time span is 35 days, starting from December 15, 2011. One column corresponds to one day.

In Fig. 3(a), specially at the ground level (0 m), we notice a regular decline of coherence moving away from the main diagonal that corresponds to the increasing time lag. Still, the observed behavior looks a bit random, showing both high and low coherence values. This behavior was found to be associated to rainfall events. For this reason, excluding rainy days is the safest option to lead this study. In fact, the rainfall effect was discussed in depth in [20], where we showed that a dramatic phase change would exactly occur in correspondence with a rainfall event. The result is presented in Fig. 3(b), in which the rainy days were flagged by setting their coherence to 0. We can see how the temporal coherence changes after 4, 17, or 27 days. We notice that the coherence value is pretty high, which is also consistent with the TropiSAR results [17]. The same temporal behavior is observed in all polarimetric channels.

In Fig. 4, we plot the coherence in a logarithmic scale versus time for the ground level in HV. The best fit line has been

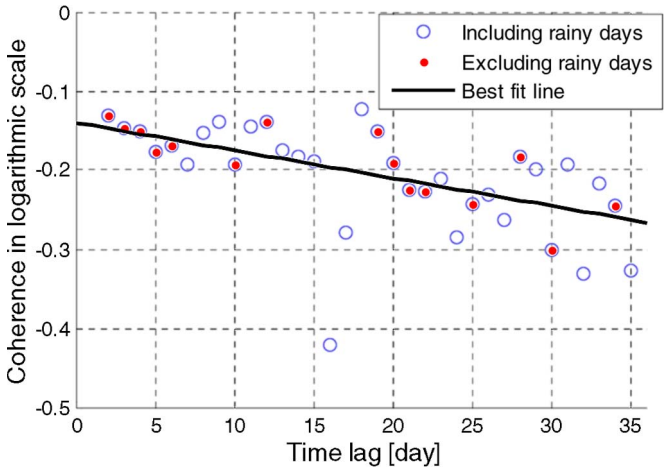

Fig. 4. Coherence in a logarithmic scale versus time for the ground level in HV. The best fit line has been performed by excluding the data set of the rainy days. The data cover the time span starting from December 15, 2011.

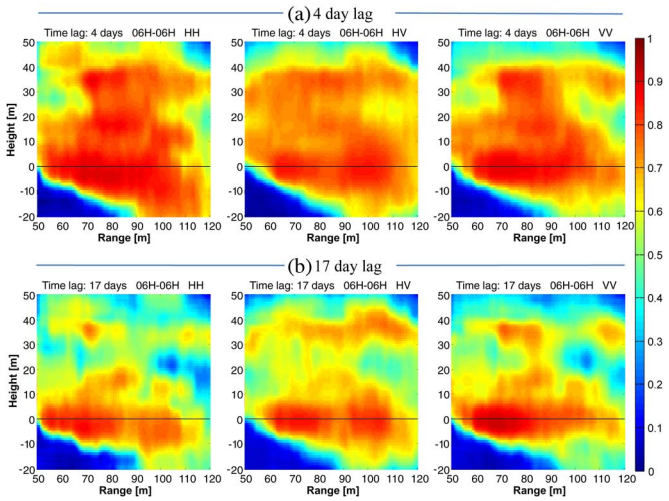

Fig. 5. (a) Dawn–dawn temporal coherence after four days. (b) Dawn–dawn temporal coherence after 17 days.

obtained by excluding the data set for rainy days, showing a linear trend. This suggests that an exponential decay can be used to quantify the temporal coherence.

IV. Temporal Decorrelation as a Function of Forest Vertical Structure

The aim of this section is to establish a link between the temporal coherence and the vertical structure by analyzing how coherence changes over time at different heights within the vegetation layer. The analysis within this section covers the time span from December 2011 to March 2012. Rainy days have been excluded from the analysis.

A. Temporal Coherence Map

Coherence estimation was carried out through both spatial and temporal averaging. Spatial averaging was performed in a space-varying fashion in order to have the same equivalent number of looks at each range and height location. Temporal averaging was carried out by taking all the pairs in the data set, spanning the same interval (e.g., all the pairs with a temporal baseline of 4 or 17 days), and by averaging their coherence to make the estimates more robust, i.e.,

$$\hat{\gamma}(nT) = \frac{\sum_{t(k_2)-t(k_1)=nT} \hat{\gamma}(k_1, k_2)}{\sum_{t(k_2)-t(k_1)=nT} 1} \tag{1}$$

where $t(k)$ is the time of the kth acquisition.

The estimated coherence maps at 4 and 17 days are reported in Fig. 5. The coherence at four days is observed to be remarkably high both at the ground and canopy levels. Passing from 4 to 17 days, the ground coherence is observed to stay high, whereas the volume coherence tends to decrease, therefore indicating coherence sensitivity to height.

B. Temporal Decorrelation Modeling

The observed behavior of the temporal coherence versus time suggests that it can be effectively modeled as an exponential decay with an initial value and a time constant, as discussed in [7]. The time constant provides an idea of the lifetime of scatterers, whereas the initial value accounts for short time changes.

We assume that the elemental scatterers in the resolution cell suddenly change their reflectivity, passing from complete coherence to zero. Once a start time is set $(t_0 = 0)$, the scatterers are divided into two classes, i.e., those that have experienced at least one change and those that have not. The model can be simply written as follows:

$$\gamma(nT) = \gamma_0 e^{-nT/\tau_0}. \tag{2}$$

γ_0, which is the initial coherence, ranges from 1 to 0 and represents the fraction of the scatterers that did not suffer from a "quick decorrelation" mechanism, and τ_0 is the time constant.

C. Expected Temporal Coherence

The retrieved model parameters γ_0 and τ_0 for the different layers are summarized in Table I. The model-fitting quality value, which is the average absolute difference between the coherence model that is identified and the coherence samples, is found to be about 0.01.

Based on this analysis, the temporal coherence at the ground level is expected to stay high at about 0.8 at 27 days. The coherence at the canopy height is expected to be about 0.8 at 4 days and about 0.65 at 27 days.

V. Conclusion

In this letter, tomographic processing has been aimed at investigating the link between the variation of temporal decorrelation over time and the forest vertical structure at P-band. Temporal coherence was then investigated by analyzing the time series that is composed by multiple tomographic snapshots.

Concerning the temporal coherence of one day, the most relevant phenomenon is the coherence drop during daytime, which is due to the effect of the wind moving the forest

TABLE I
RETRIEVED MODEL PARAMETERS: INITIAL COHERENCE γ_0 AND TIME CONSTANT τ_0

Layer	HH		HV		VV	
	γ_0	τ_0 (day)	γ_0	τ_0 (day)	γ_0	τ_0 (day)
0 m	0.94±0.01	160±7	0.90±0.01	166±2	0.94±0.01	190±2
10 m	0.91±0.01	107±7	0.86±0.01	112±4	0.88±0.01	122±5
20 m	0.84±0.01	101±9	0.80±0.01	118±5	0.79±0.01	101±5
30 m	0.84±0.02	120±10	0.80±0.02	128±8	0.78±0.03	124±11

canopy. This result already appears to provide a very useful input concerning the BIOMASS mission, as it suggests that the performance over a tropical forest could be optimized by gathering acquisitions in early morning or night hours. For this reason, the long-term temporal decorrelation has been evaluated considering dusk or dawn.

Long-term coherence was analyzed by considering the periods from November 2011 to March 2012. We decided to focus on the dawn–dawn acquisitions rather than the dusk–dusk acquisitions since the ionospheric disturbances are more severe at dusk. The analysis has shown that the estimated temporal behavior does change within the forest volume, i.e., the highest coherence values are observed at the ground level. The temporal coherence at the ground level is expected to stay high at about 0.8 at 27 days, whereas the coherence at the canopy height is expected to be about 0.8 at 4 days and about 0.65 at 27 days. We remark that rainy days have been excluded from the analysis. Whether it is possible to get good results in the presence of rainy acquisitions is an open point. Future works will consider the treatment of rainfall events and the simulation of the impact of temporal decorrelation on BIOMASS tomography.

ACKNOWLEDGMENT

The authors would like to thank the Eurpoean Space Agency and Centre National d'Etudes Spatiales (CNES) for supporting the TropiScat experiment, R. Bianchi for providing useful insights and discussions, and L. Blanc and B. Burban of Ecologie des Forets de Guyane, and D. Bonal of the Institut National de la Recherche Agronomique for their welcome and help with the Guyaflux tower.

REFERENCES

[1] Report for mission selection: BIOMASS, European Space Agency, Paris, France, ESA SP-1324/1. [Online]. Available: http://esamultimedia.esa.int/docs/EarthObservation/SP1324-1_BIOMASSr.pdf

[2] T. Le Toan, S. Quegan, M. Davidson, H. Balzter, P. Paillou, K. Papathanassiou, S. Plummer, F. Rocca, S. Saatchi, H. Shugart, and L. Ulander, "The BIOMASS mission : Mapping global forest biomass to better understand the terrestrial carbon cycle," *Remote Sens. Environ.*, vol. 15, no. 11, pp. 2850–2860, Jun. 2011.

[3] *Article 5 (Frequency Allocations) of the Radio Regulations*, ITU-2004, International Telecommunication Union, Geneva, Switzerland, 2004.

[4] S. Quegan and J. Lamont, "Ionospheric and tropospheric effects on synthetic aperture radar performance," *Int. J. Remote Sens.*, vol. 7, no. 4, pp. 525–539, Apr. 1986.

[5] S. Quegan, J. Green, R. Zandona-Schneider, R. Scheiber, and K. Papathanassiou, "Quantifying and correcting ionospheric effects on P-band SAR images," in *Proc. IEEE IGARSS*, Jul. 2008, vol. 2, pp. II-541–II-544.

[6] J. S. Kim, K. Papathanassiou, S. Quegan, and N. Rogers, "Estimation and correction of scintillation effects on spaceborne P-band SAR images," in *Proc. IEEE IGARSS*, Jul. 2012, pp. 5101–5104.

[7] F. Rocca, "Modeling interferogram stacks," *IEEE Trans. Geosci. Remote Sens.*, vol. 45, no. 10, pp. 3289–3299, Oct. 2007.

[8] H. A. Zebker and J. Villasenor, "Decorrelation in interferometric radar echoes," *IEEE Trans. Geosci. Remote Sens.*, vol. 30, no. 5, pp. 950–959, Sep. 1992.

[9] F. Lombardini and M. Pardini, "Superresolution differential tomography: Experiments on identification of multiple scatterers in spaceborne SAR data," *IEEE Trans. Geosci. Remote Sens.*, vol. 50, no. 4, pp. 1117–1129, Apr. 2012.

[10] D. Reale, G. Fornaro, A. Pauciullo, X. Zhu, and R. Bamler, "Tomographic imaging and monitoring of buildings with very high resolution SAR data," *IEEE Geosci. Remote Sens. Lett.*, vol. 8, no. 4, pp. 661–665, Jul. 2011.

[11] S.-K. Lee, F. Kugler, K. Papathanassiou, and I. Hajnsek, "Quantification of temporal decorrelation effects at L-Band for polarimetric SAR interferometry applications," *IEEE J. Sel. Topics Appl. Earth Observ. Remote Sens.*, vol. 6, no. 3, pp. 1351–1367, Jun. 2013.

[12] M. Lavalle, M. Simard, and S. Hensley, "A temporal decorrelation model for polarimetric radar interferometers," *IEEE Trans. Geosci. Remote Sens.*, vol. 50, no. 7, pp. 2880–2888, Jul. 2012.

[13] I. Hajnsek, R. Scheiber, L. Ulander, A. Gustavsson, G. Sandberg, S. Tebaldini, A. Monti Guarnieri, F. Rocca, F. Lombardini, and M. Pardini, "BioSAR 2007. Technical assistance for the development of airborne SAR and geophysical measurements during the BioSAR 2007 experiment: Final report without synthesis," ESA, Paris, France, ESA contract 20755/07/NL/CB, 2008.

[14] S. Tebaldini, M. Mariotti d'Alessandro, D. Ho Tong Minh, and F. Rocca, "P band penetration in tropical and boreal forests: Tomographical results," in *Proc. IEEE IGARSS*, Jul. 2011, pp. 4241–4244.

[15] S. Tebaldini and F. Rocca, "Multibaseline polarimetric SAR tomography of a boreal forest at P- and L-bands," *IEEE Trans. Geosci. Remote Sens.*, vol. 50, no. 1, pp. 232–246, Jan. 2012.

[16] D. Ho Tong Minh, T. Le Toan, F. Rocca, S. Tebaldini, M. Mariotti d'Alessandro, and L. Villard, "Relating P-band synthetic aperture radar tomography to tropical forest biomass," *IEEE Trans. Geosci. Remote Sens.*, vol. 52, no. 2, pp. 967–979, Feb. 2014.

[17] P. C. Dubois-Fernandez, T. Le Toan, S. Daniel, H. Oriot, J. Chave, L. Blanc, L. Villard, M. W. J. Davidson, and M. Petit, "The TropiSAR airborne campaign in French Guiana: Objectives, description, and observed temporal behavior of the backscatter signal," *IEEE Trans. Geosci. Remote Sens.*, vol. 50, no. 8, pp. 3228–3241, Aug. 2012.

[18] C. Albinet, P. Borderies, T. Koleck, F. Rocca, S. Tebaldini, L. Villard, T. Le Toan, A. Hamadi, and D. Ho Tong Minh, "TropiScat: A ground based polarimetric scatterometer experiment in tropical forests," *IEEE J. Sel. Topics Appl. Earth Observ. Remote Sens.*, vol. 5, no. 3, pp. 1060–1066, Jun. 2010.

[19] D. Ho Tong Minh, F. Rocca, S. Tebaldini, M. Mariotti d'Alessandro, and T. Le Toan, "Linear and circular polarization P band SAR tomography for tropical forest biomass study," in *Proc. 9th EUSAR Conf.*, Apr. 2012, pp. 489–492.

[20] D. Ho Tong Minh, S. Tebaldini, F. Rocca, T. Koleck, P. Borderies, C. Albinet, L. Villard, A. Hamadi, and T. Le Toan, "Ground-based array for tomographic imaging of the tropical forest in P-band," *IEEE Trans. Geosci. Remote Sens.*, vol. 51, no. 8, pp. 4460–4472, Aug. 2013.

[21] D. Bonal, A. Bosc, S. Ponton, J. Goret, B. Burban, P. Gross, J. Bonnefond, J. Elbers, B. Longdoz, D. Epron, J. Guehl, and A. Granier, "Impact of severe dry season on net ecosystem exchange in the neotropical rainforest of French Guiana," *Glob. Change Biol.*, vol. 14, no. 8, pp. 1917–1933, Aug. 2008.